Acoustic Emission Characteristics of Gas-Containing Coal during Loading Dilation Process

Z. Q. Yin[1, 2,*], G. X. Xie[1, 2], L. Wang[1, 2], Z. X. Hu[1, 2] and Y. Zou[3]

[1]*The Provincial Key Laboratory of mining effects & disasters preventing under deep mining in Anhui, Anhui University of Science and Technology, Huainan, 232001-China*
[2]*Sch. of Mineral & Safety, Anhui University of Science and Technology, Huainan, 232001, China*
[3]*Lab. for Rock Mechanics (LMR), École polytechnique fédérale de Lausanne (EPFL), Lausanne, CH 1015, Switzerland*

Abstract

Raw coal was used as the study object in this paper to identify the evolution characteristics of acoustic emission (AE) during the dilation process of gas-containing coal. The coal specimens were stored in gas seal devices filled with gas at different pressures (0, 0.5, 1.0, and 1.5 MPa) for 24 h prior to testing. Then, the specimens were tested in a rock-testing machine, and the deformation and crack fracture patterns were recorded by using strain gauges and an AE system. The axial and volumetric strains–stress curves were analyzed in relation to the AE and the failure mode. Results show that as gas pressure increases, the uniaxial compression strength and elasticity modulus of gas-containing coal decreases, whereas the Poisson's ratio increases. In all the coal specimens, the dilation initiation stress decreases, and the dilation degree increases. During the dilation process, before the loaded coal specimens reach peak stress, and as the load increases, the changes in the specimens and in the AE energy parameter of specimens can be divided into four phases: crack closure deformation, elastic deformation, stable crack propagation, and unstable crack propagation (dilation process). Across the four phases, the AE energy increases evidently during crack closure and elastic deformation but decreases during stable crack propagation. As the gas pressure increases, the AE signal frequency increases from 4.5 KHz to 8.1 KHz during the dilation process. Thus, the gas presence in coal specimens exerts a significant influence on the closure of sample cracks and dilation damage.

Keywords: Dilation initiation stress; Gas-containing coal; Acoustic emission; Energy; Signal frequency

---

1. Introduction

At deep mining depths, the development of deep coal resources is affected by the weight of covering rocks, mining-induced stress, and the high gas pressure contained within coal seams [1]. Many field and experimental studies show that coal and gas outbursts are caused by the co-influences of ground stress, gas stress, and the mechanical characteristics of coal and rocks. The damage resulting from the unstable state of gas-containing coal is one of the causes of coal and gas outburst disasters. Understanding the damaging and unstable mechanisms of gas-containing coal is the key to predicting gas outburst accidents, and determining the acoustic emission (AE) characteristics of the gas-containing coal during the damage process is an effective way to assess whether the obtained gas-containing coal is unstable and damaged [2–3]. Therefore, research on the AE characteristics of gas-containing coal and the mechanisms of its damaging and unstable process is useful in predicting and assessing coal and gas outburst accidents.

Numerous studies focused on the unstable process in coal and rocks. However, many of these studies concentrated on gas-containing coal creep deformation, gas seepage characteristics, and the AE characteristics during the unstable process in coal or rocks without gas, rock slope, sandstone, and limestone, among others [4–6]. Some scholars have made innovative attempts by conducting empirical studies on gas-containing coal and obtained some significant results. Ranjith [7] used AE devices to monitor the breaking and damage process in coal after CO_2 absorption; compared with natural conditions, CO_2 absorption by coals increased the stress ratio compared with the peak during the development and extension of cracks. However, the opposite occurred when the cracks are damaged. Zhao [8] and Meng [9] conducted AE experiments on gas-containing coal under triaxial compression and established a damage deformation model of gas-containing coal based on AE characteristics. Liu [10] employed a fractal theory to discuss the evolutional law of related AE dimensions in the damage process of gas-containing coal.

Previous studies that conducted mechanical experiments on gas-containing coal are still in the exploration stage because of limited equipment and methods. Few studies focused on crack expansion and AE evolution in gas-containing coal from loading to becoming unstable to becoming damaged. This paper presents a laboratory investigation on the characterization of the failure patterns and damage mechanisms of gas-containing coal by integrating the use of strain gauges and AE monitoring technology. The fracture behavior and energy release of raw coal were recorded by the strain gauges and AE under axial

---

loading and effects of gas adsorbing on the strength and failure mechanics of raw coal.

2. Experimental Method

2.1 Sample Preparation
All coal specimens used in the experiment were obtained from the 11426 working face of the Xieqiao Mine in Huainan area in China. All selected specimens were free from visible uneven structures or defects. To reduce the influence of the bedding surface on the strength of the specimens, coal blocks were drilled in the axial direction, with the drilling machine positioned vertical to the bedding surface. Furthermore, both ends and side faces of the specimens were ground carefully as required to measure the physical and mechanical characteristics of the coal. Then, the size of the coal specimens was set to 25 mm × 25 mm × 50 mm, and both the non-parallelism and non-perpendicularity of the specimens were less than 0.02 mm.

2.2 Experimental Equipment
As shown in Fig. 1, the gas-containing coal experimental system consisted of three devices: gas seal device, gas supply device, and data collection device. The gas seal device was connected to the gas supply device through an air pipeline. To control gas pressure to ensure that the specimens were in a stable state, two testing holes were prepared in the gas seal device, and the two holes were connected to the static strain indicator and AE device through wires. Then, data were collected during the loading process.
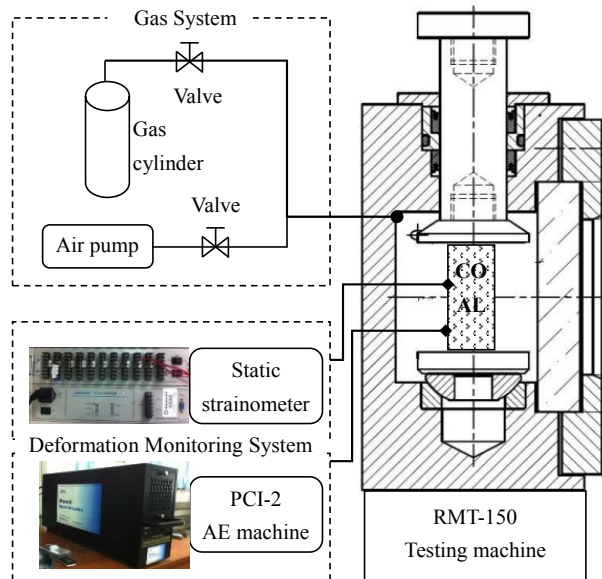

Fig. 1. Testing system of coal absorbed gas

Two strain gauges (BX120-2AA) were used for the strain measurement. The gauges were installed in the circumferential and axial directions on all coal specimens to measure the lateral strain (ε_l) and axial strain (ε_a) of the specimens during the loading process. The strain history of strain gauges that were connected to the high-speed static strain indicator (YE2539) was recorded, thereby enabling the identification of the stress thresholds for crack closure, stable propagation, and unstable propagation. Strain data

collection was conducted twice per second. The volume strain (ε_v) of the specimens can be calculated by using the following formula:

$$\varepsilon_v = \varepsilon_a + 2\varepsilon_l \tag{1}$$

The AE monitoring system used for this experiment is called the PCI-2 6 channel data acquisition system (Micro-II). A PICO resonant sensor was attached on the center of the sample surface. The AE data was collected during the loading process. As shown in Fig. 2, the AE sensor and strain gauges were connected to the external equipment through wires inside the gas-sealing bolts.
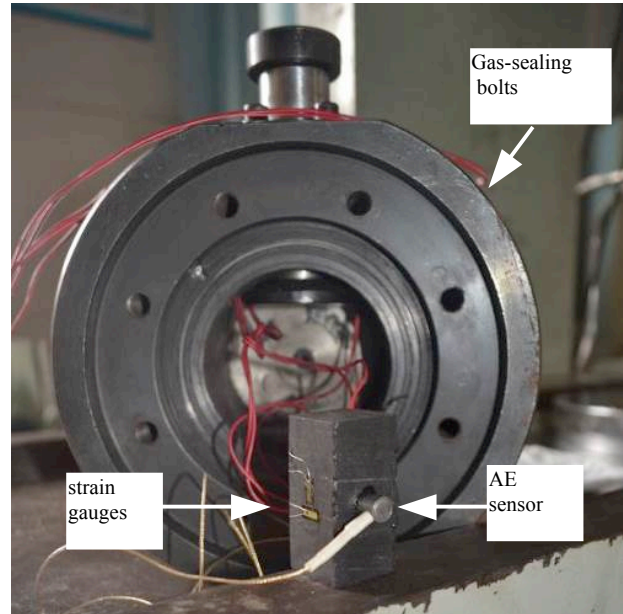

Fig. 2. Coal specimens with installed strain gauges and AE sensor

2.3 Experimental Process
In this study, the specimens that do not absorb gas were selected as the control tests, and five samples were selected to determine the mechanical parameters of the raw coal. Five replicas were selected for each condition and with gas (0.5, 1.0, and 1.5 MPa) using the gas seal device at room temperature (26 ºC) for 24 h. For the test, the axial loading was conducted by using a universal rock-testing machine (RMT-150). The axial loading was assisted by the displacement control, and the loading rate was 0.1 mm/min. Once the specimens had been saturated, axial load was applied to the sample by using the testing machine, and deformation and AE signals were recorded simultaneously by using the strain gauges and the AE equipment.

3. Experimental Discussion

3.1 Characteristics of Sample Deformation and Strength
Fig. 3 shows the typical uniaxial stress–strain curves of the coal and rock specimens at gas pressures of 0, 0.5, 1.0, and 1.5 MPa. Figure 3 shows that the peak stress and volume deformation of the specimens are significantly influenced by gas pressure. As shown in Table 1, by analyzing the stress–strain curves, the elasticity modulus and Poisson's ratio of the different specimens can be calculated.
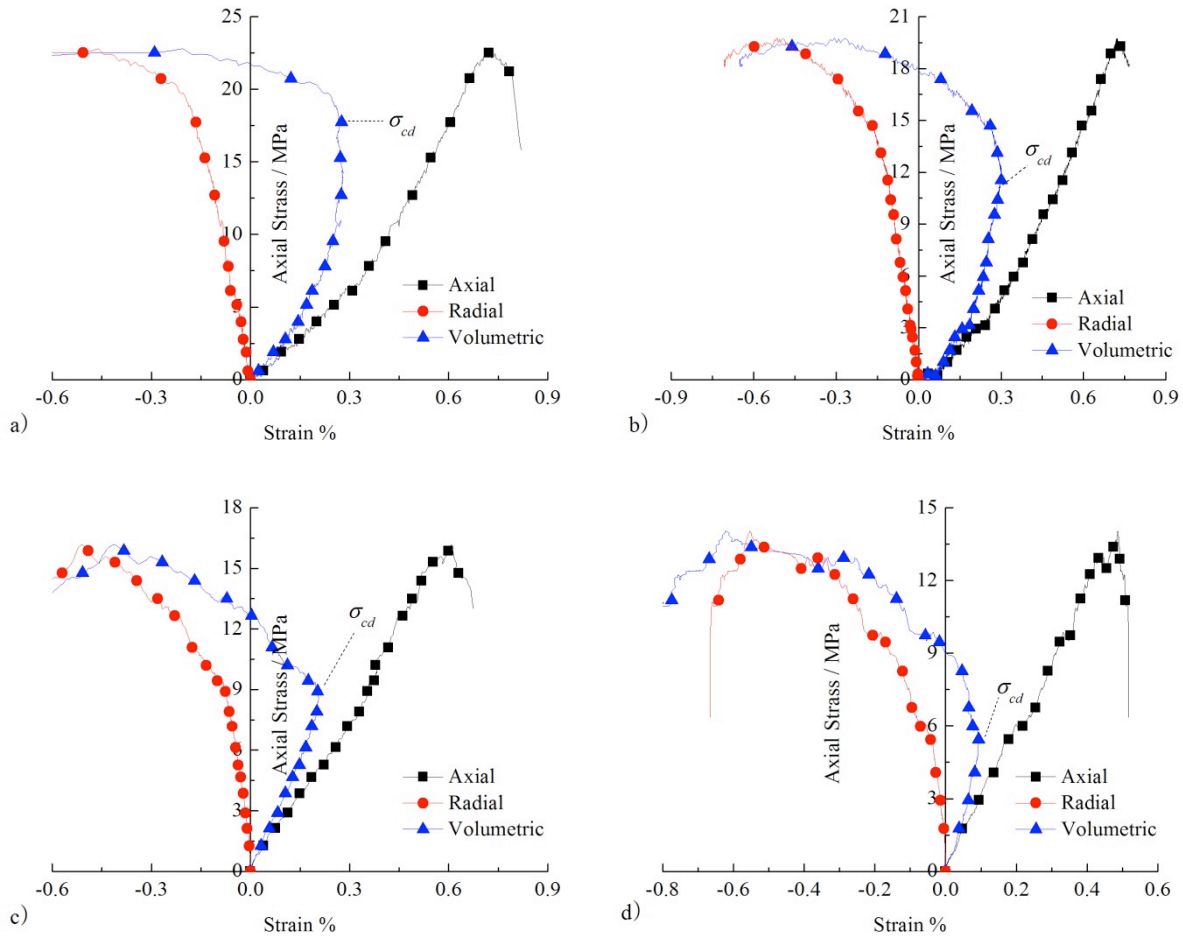
Fig. 3. Stress–strain curves for tested specimens. (a) 0MPa, (b)1.0MPa, (c)1.5MPa, (d)2.0MPa

Table 1 Mean values of uniaxial compressive strength (UCS), Young's modulus (*E*) and Poisson's ratio obtained from testing and changes in these values relative to values obtained from testing of the no gas absorbed sample

Specimen	UCS (MPa)	Average UCS	Δ UCS (%)	Young's Modulus (GPa)	Average E	Δ E (%)	Poisson's ratio	Average Poisson's ratio
No gas								
1	22.79			4.10			0.22	
2	24.66			4.43			0.25	
3	20.51	23.54		3.45	4.05		0.21	0.24
4	27.85			3.89			0.24	
5	21.88			4.37			0.26	
0.5MPa								
1	19.73			3.83			0.20	
2	23.20			3.56			0.25	
3	20.68	19.70	-16.31	3.02	3.48	-14.07	0.27	0.25
4	18.90			3.90			0.31	
5	15.96			3.09			0.23	
1.0MPa								
1	16.12			2.81			0.23	
2	12.61			3.25			0.27	
3	13.40	15.71	-33.26	3.42	2.82	-30.37	0.28	0.28
4	18.81			2.47			0.32	
5	17.64			2.15			0.29	
1.5MPa								
1	14.04			2.75			0.27	
2	17.80			2.17			0.35	
3	12.26	13.75	-41.58	3.19	2.72	-32.83	0.23	0.30
4	9.03			2.55			0.33	
5	15.62			2.94			0.32	

The statistics presented in Table 1 shows that the variable coefficients (the ratio between the standard deviation and the mean value) of various parameter strengths range from 12 to 30. Although the various measured mechanical performance indicators vary, some laws for

mean values still apply. With increasing gas pressure, the compressive strength of gas-containing coal specimens decreases. When gas pressure reaches 1.5 MPa, the compressive strength declines from 23.54 MPa to 13.75 MPa, which is a reduction rate of 41.58%. The elasticity

modulus, which is another important parameter that reflects the mechanical characteristics of coal specimens, exhibits a similar trend. Table 1 shows that the elasticity modulus of coal specimens decreases as the gas pressure increases. When gas pressure reaches 0.5, 1.0, and 1.5 MPa, the elasticity modulus is reduced by 14.07%, 30.37%, and 32.83%, respectively. By contrast, the Poisson's ratio increases as the gas pressure increases. When the compression strength of the coal specimens is reduced, the plasticity increases.

Fig. 3 shows that the total volume of the coal specimens is compressed and then starts expanding because of the effect of axial stress. The initiation point is when the volume of the specimens changes from being compressed to expanding; the corresponding axial stress is the dilation initiation stress (DIS) σ_{cd}; with the effect of gas occurrence, the dilation of specimens shows clear differences and the DIS tends to reduce, but the dilation degree increases.

3.2 Crack Expansion and Acoustic Emission
From a macro viewpoint, the dilation phenomenon occurs because specimens are affected by the external load and the cracks of internal particles appear, expand, and combine. The dilation volume includes the volumetric strain of crack volume and elasticity volumetric strain of specimens. The elasticity volumetric strain (ε_{ve}) can be calculated by using the following formula:

$$\varepsilon_{ve} = \sigma \ (1 - 2v) \ / \ E \tag{2}$$

where σ is the axial stress, v is the Poisson's ratio, and E is the Young's modulus.

Therefore, the crack volumetric strain (ε_{vc}) of specimens can be calculated by using the following formula:

$$\varepsilon_{vc} = \varepsilon_v - \varepsilon_{ve} \tag{3}$$

Moreover, the crack volumetric strain reflects the micro change of cracks, from being affected by strain and from being closed to being damaged.

The main monitoring parameters in AE monitoring are ring count, energy, absolute energy, strength of signals, amplitude, and frequency [11-13]. Energy can reflect the relative energy or strength of AE cases, whereas frequency can reflect the material properties of AE signals; both parameters are often used by most researchers on loaded coal and rock AE characteristics [14]. In this paper, energy and frequency are used to analyze AE characteristics of gas-containing coal and their evolution principles.

In Fig. 4, with the change of loaded cracks, the AE energy also changes in the uniaxial compression damage process with non-gas-containing coal and gas-containing coal.
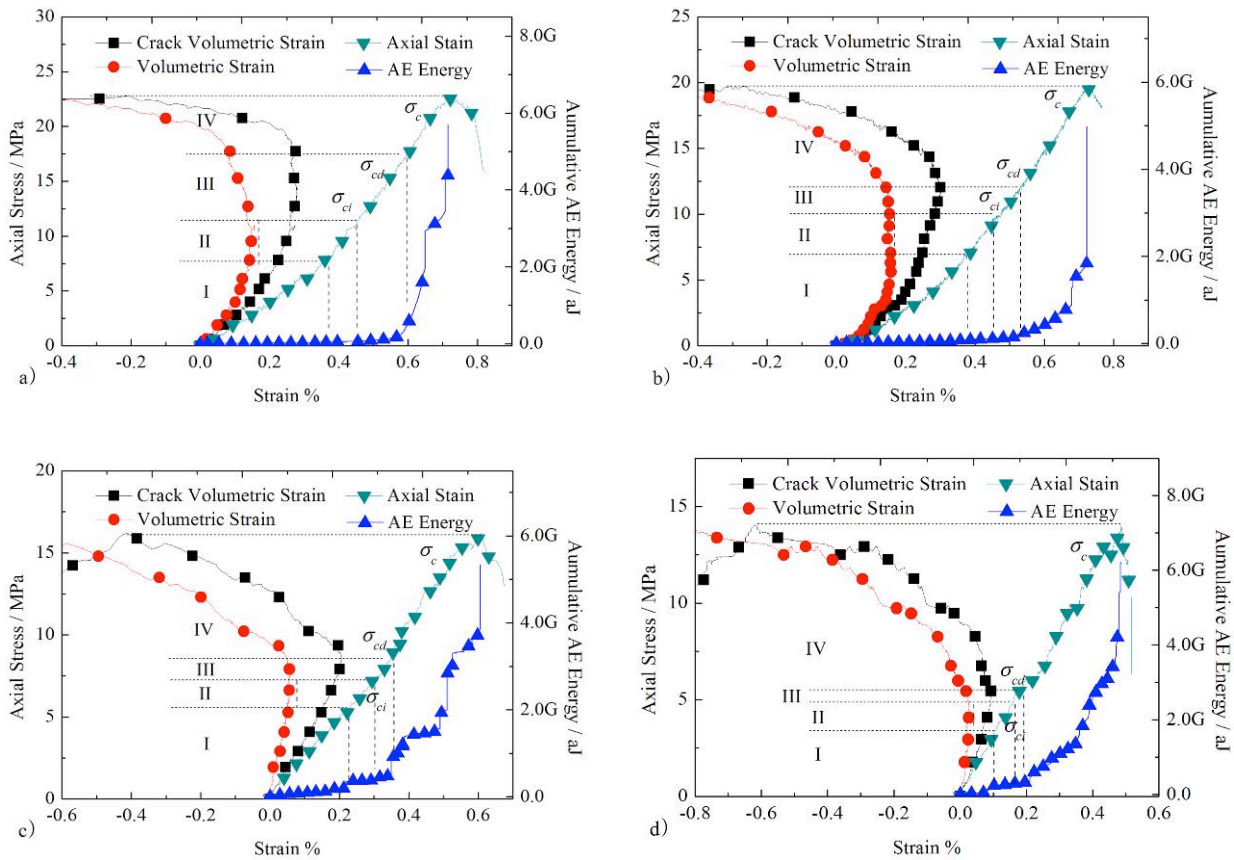

Fig. 4. AE parameters of coal in process dilation of under triaxial compression. (a) 0MPa, (b)1.0MPa, (c)1.5MPa, (d)2.0MPa

In Fig. 4, based on the crack volumetric strain curve and accumulated energy of AE, with the increase in axial stress, the volume of coal cracks tends to be crack-closure deformation, elastic deformation, stable crack propagation, and unstable crack propagation. With the effect of axial stress, crack-closure deformation occurs initially; when the closure reaches a certain degree, the specimens will exhibit elasticity deformation, and the corresponding axial stress is

the initial stress of elasticity σ_{cc}. Then, cracks shift from linear elasticity to stable crack propagation, and the corresponding axial stress is crack initiation stress (CIS) σ_{ci}. When the specimens enter a state of unstable crack propagation, the specimens will exhibit obvious dilation, and the corresponding axial stress is considered unstable dilation stress of cracks (DIS) σ_{cd}. Table 2 presents CIS σ_{ci}, dilation initiation stress σ_{cd}, and peak stress σ_c.

Table 2 shows that with the increase in gas pressure, the CIS gradually reduces from 10.93 MPa to 4.73 MPa; meanwhile, in the loading process, the strain in the crack dilation phase reduces from 6.79 MPa to 0.86 MPa. When gas pressure inside the coal absorbed gas increases and the CIS reduces, adding a small strain can cause cracks inside the coal specimens; a shift from cracking to unstable dilation occurs, which indicates that gas can strengthen the dilation of cracks of loaded coal specimens.

Fig. 4 indicates that the four phases of crack evolution and the AE energy are obviously influenced by gas pressure. The AE energy in different phases is calculated in Table 3.

Table 3 indicates that when the gas pressure increases to 1.5 MPa, the total AE energy and AE energy of unstable dilation of cracks increase. Meanwhile, the AE energy in the stable dilation phase gradually reduces from 0.330 J to 0.058 J. This finding reflects that the AE energy is influenced by gas, and the cracks change from crack initiation to unstable dilation fracture state rapidly. At the same time, the AE energy in the closed phase of cracks gradually increases from 0.043 J to 0.237 J. This finding reflects that with an increase in gas pressure, the closure degree increases in cracks during the compressed and closed phases, and the raw coal specimens that have absorbed gas fully demonstrate evident stress–strain densification.

3.3 Energy characteristics in fracture process
The energy absorption (U) of coal sample in the principle stress is given by [15]:

$$U = \int_0^{\varepsilon_1} \sigma_1 d\varepsilon_1 + \int_0^{\varepsilon_2} \sigma_2 d\varepsilon_2 + \int_0^{\varepsilon_3} \sigma_3 d\varepsilon_3 \qquad (4)$$

Where σ_1, σ_2, σ_3, ε_1, ε_2, ε_3 are principle stresses and strains respectively.

According to the first law of thermodynamics, the energy absorption (U) is defined as:

$$U = U_d + U_e \qquad (5)$$

Where U_d is the dissipated energy in the creation of damaged deformation, U_e is elastic energy stored in the coal sample released when the coal sample is broken.
The elastic energy stored, as follows [16]:

$$U_e = \frac{1}{2E}\left[\sigma_1^2 + \sigma_2^2 + \sigma_3^2 - 2v(\sigma_1\sigma_2 + \sigma_2\sigma_3 + \sigma_1\sigma_3)\right] \qquad (6)$$

From Eq. (1) to Eq. (3), the dissipated energy in the uniaxial compression tests, as follows:

$$U_d = U - U_e = \int_0^{\varepsilon_1} \sigma_1 d\varepsilon_1 - \frac{1}{2E}\sigma_1^2 \qquad (7)$$

Table 4 shows the strain energy at crack initiation point, dilation initiation point and peak point. The results indicate that energy absorption, dissipated energy and elastic energy decrease with increasing gas pressure.

Fig. 5 shows the AE energy and the strain energy at the crack initiation point and the peak point (from Tables 3 and 4). Dissipated energy decreases linearly with increasing gas pressure, but the AE energy increases.

As shown in Table 3 and Fig. 5, AE energy increases with the increase in gas pressure. The absorbed energy of the loaded coal samples is used to form new fragment surfaces and released AE energy; high AE energy indicates that more cracks are created in the same sample. Therefore, high AE energy corresponds to high dissipated energy of the coal sample. The changing law of the absorption energy with gas pressure is the opposite of the law of AE energy with gas pressure, which also decreases with gas pressure. Therefore, higher gas pressure with low energy loaded from the external environment can further lead to severe coal damage.

3.4 Characteristics of Acoustic Emission Signal Frequency
Gas not only affects the mechanical parameter, stress–strain curve, and AE energy, but also has obvious influence on the AE signal frequency characteristics in the process of coal absorbed gas being damaged and becoming unstable. Fig. 6 shows that the laws on the AE signal frequency vary with the change in gas pressure in the full stress–strain loading process.

Fig. 6 indicates that the initial AE signals are at a low frequency (around 1 KHz) when no gas appears and with increasing strain. When the strain is greater than the initiation stress of dilation and enters the dilation phase with the dilation of cracks, high-frequency AE signals (around 4.5 KHz) occur; the frequency of AE signals is highest (11.7 KHz) when the stress passes the peak, and the specimens are destroyed. When the loaded stress is smaller than the dilation stress with the increase in gas pressure, the times and strength of generating high-frequency signals increases gradually. Fig. 7 shows the calculation of AE signal frequency of coal in the damage and dilation phase after passing the peak and under different gas pressures.

Table 2 Mean values of uniaxial compressive strength (UCS), dilation initiation stress (DIS) and crack initiation stress (CIS) under different gas pressure

Test condition	UCS (MPa)	DIS (MPa)	CIS (MPa)	DIS / UCS %	CIS / UCS %	Stable crack propagation (MPa)	Unstable crack propagation (MPa)
No gas	22.79	17.72	10.93	77.78	47.96	6.79	5.07
0.5MPa	19.73	12.03	9.96	60.95	50.48	2.07	7.7
1.0MPa	16.12	8.62	7.53	53.48	46.71	1.09	7.5
1.5MPa	14.04	5.59	4.73	39.79	33.69	0.86	8.45

Table 3 AE energy parameters of coal in process fracture of under triaxial compression

Test condition	AE energy (J)	Energy of unstable crack propagation (J)	Energy of stable crack propagation (J)	Energy of elastic deformation (J)	Energy of crack closure deformation (J)
No gas	5.70	5.309	0.330	0.018	0.043
0.5MPa	4.99	4.746	0.134	0.038	0.072
1.0MPa	5.32	4.804	0.135	0.052	0.329
1.5MPa	6.22	5.620	0.058	0.019	0.237

Table 4 Strain energy corresponding to characteristic points in the loading process (J/cm^3)

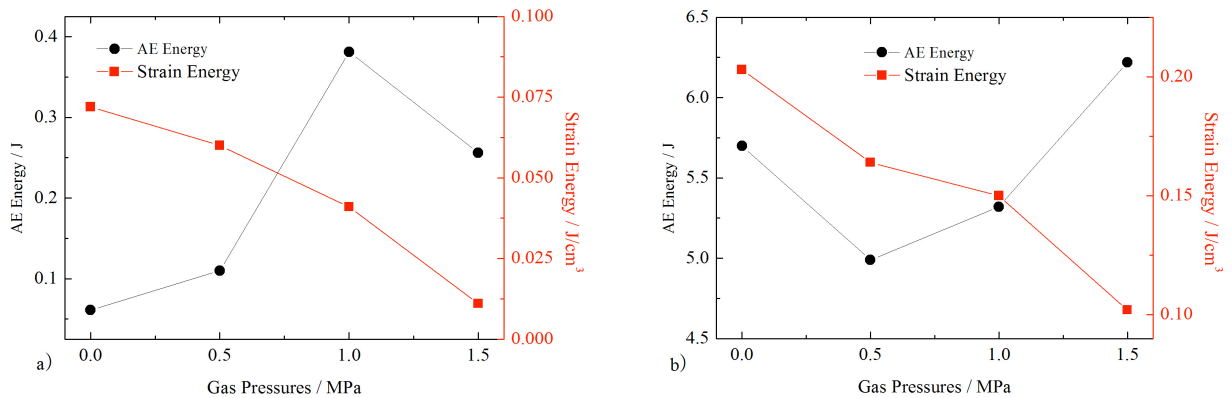| Test condition	Crack initiation point			Dilation initiation point			Peak point		
	U	U_e	U_d	U	U_e	U_d	U	U_e	U_d
No gas	0.087	0.015	0.072	0.177	0.039	0.138	0.267	0.064	0.203
0.5MPa	0.074	0.014	0.060	0.105	0.021	0.084	0.220	0.056	0.164
1.0MPa	0.051	0.010	0.041	0.062	0.013	0.049	0.196	0.046	0.150
1.5MPa	0.015	0.004	0.011	0.021	0.006	0.016	0.138	0.036	0.102

Fig. 5. AE energy and dissipated energy changing with gas pressure. (a) crack initiation point and (b) peak point
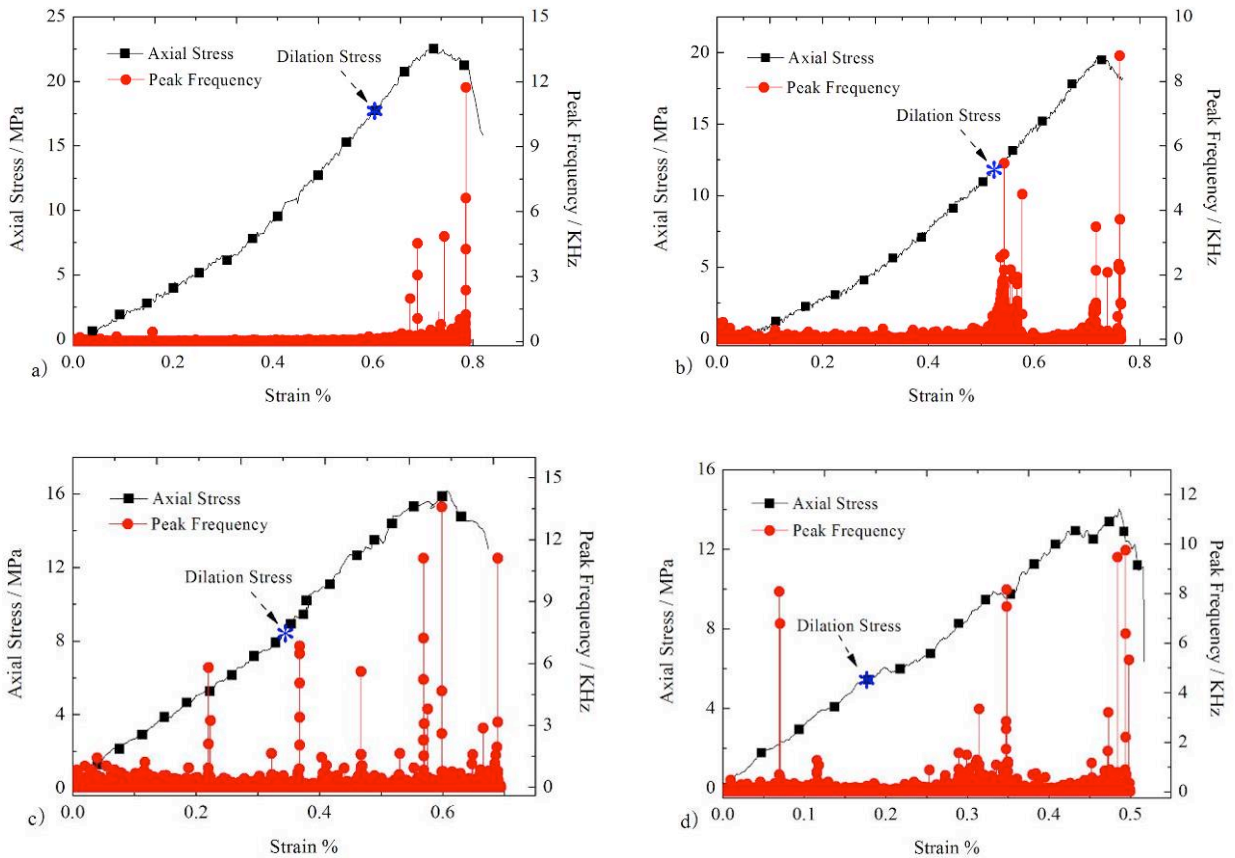

Fig. 6. The acoustic emission signal frequency of specimens under different gas pressure

With the increase in gas pressure, the AE signal frequency of coal specimens that are damaged after the peak value is between 9 and 13 KHz, which is less affected by absorbed gas. However, the AE signal frequency evidently increased in the dilation phase from 4.5 KHz to 8.1 KHz. In accordance with related literature for materials such as rock, when such materials are loaded with strain, a low-intensity microcrack exists, and the structure is balanced; the AE signals are mostly at a low frequency. However, when a high-intensity microcrack exists and the structure is damaged, the AE signals are mostly at a high frequency [17, 18]. Therefore, with the increase in gas pressure, the possibility of coal sample being damaged in the structure increases under low strain.
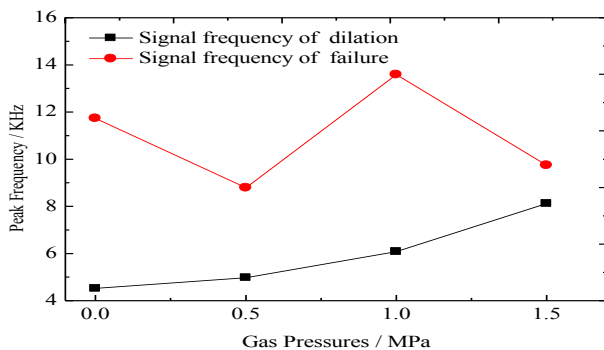

Fig. 7. The AE signal frequency of specimens on dilation and failure phase

4. Conclusion

With the comprehensive influence of gas state in free and absorbed states, the structure of coal absorbed gas changes.

Gas not only weakens the peak strength and elasticity modulus of coal, changes the shape of the full stress–strain curve, reduces the initiation stress of dilation, and increases the dilation degree, but also transforms the AE characteristics of coal absorbed gas in the damaged and unstable states.

The dissipated energy decreases with the increase in gas pressure, but the AE energy increases. The AE energy of gas-containing coal has a positive correlation with gas pressure in the densification and unstable dilation phases of cracks; it also has a negative correlation with gas pressure in the stable dilation phase. The initiation stress of cracking reduces with increasing gas pressure, the condition of cracks inside coal specimens can transform from crack initiation to unstable expansion with lower stress difference.

Gas pressure has no obvious influence on the AE signals that are generated after the peak stress of the coal specimens is damaged. The frequency of the AE signals increase significantly from 4.5 KHz to 8.1 KHz with the increase in gas pressure in the dilation phase. The aggravation effects of gas on the damage process of loaded coal specimens are further proved by the above finding.

References

1. Xie, G. X., Hu, Z. X., Wang, L., "Coal mining dilatancy characteristics of high gas working face in the deep mine", *Journal of China Coal Society*, 39(1) , 2014, PP. 91-96. (in Chinese)
2. He, X., Nie, B., Chen, W., Wang, E., Dou, L., Wang, W., Liu, M., Hani, M., "Research progress on electromagnetic radiation in gas-containing coal and rock fracture and its applications", *Safety Science*, 50(4), 2012, PP. 728-735.
3. Liu, H., Liu, H., Cheng, Y., "The elimination of coal and gas outburst disasters by ultrathin protective seam drilling combined with stress-relief gas drainage in Xinggong coalfield", *Journal of Natural Gas Science and Engineering*, 21(6), 2014, PP. 837-844.
4. Mogi, K., "Study of elastic shocks caused by the fracture of heterogeneous materials and its relations to earthquake phenomena", *Bulletin of the Earthquake Research Institute*, 40(1), 1962, PP. 125-173.
5. Yang, S. Q., Jin, H. W., "Strength failure and crack coalescence behavior of brittle sandstone samples containing a single fissure under uniaxial compression", *International Journal of Fracture*, 168(2), 2011, PP. 227-250.
6. Cheon, D. S., Jung, Y. B., Park, E. S., Song, W. K., Jang, H. I., "Evaluation of damage level for rock slopes using acoustic emission technique with waveguides", *Engineering Geology*, 121(1–2), 2011, PP. 75-88.
7. Ranjith, P. G., Jasinge, D., Choi, S. K., Mehic. M., Shannon, B., "The effect of CO2 saturation on mechanical properties of Australian black coal using acoustic emission", *Fuel*, 89(3), 2010, PP. 2110-2117.
8. Zhao, H. B., Yin, G. Z., "Study of acoustic emission characteristics and damage equation of coal absorbed gas", *Rock and Soil Mechanics*, 32(3), 2011, PP. 667-671. (in Chinese)
9. Meng, L., Wang, H. W., Li, X. H., Zhao, Y. X., "Investigation on acoustic emission characteristics in failure process of coal absorbed methane", J*ournal of China Coal Society*, 39(2), 2014, PP. 377-383. (in Chinese)
10. Liu, Y. B., Cao, S. G., LI. Y., Guo, P., Zhang, Z. G., "Correlation dimension analysis of AE sequence under failure process of gas-filled coal", *Journal of Chongqing University*, 35(3), 2012, PP. 108-114. (in Chinese)
11. Karakus, M., Perez, S., "Acoustic emission analysis for rock–bit interactions in impregnated diamond core drilling", *Journal of Rock Mechanics and Geotechnical Engineering*, 68, 2014, PP. 36-43.
12. Aker, E., Kühn, D., Vavryčuk, V., Soldal, M., Oye, V., "Experimental investigation of acoustic emissions and their moment tensors in rock during failure", *Journal of Rock Mechanics and Geotechnical Engineering*, 70, 2014, PP. 286-295.
13. Khazaei, C., Hazzard, J., Chalaturnyk, R., "Damage quantification of intact rocks using acoustic emission energies recorded during uniaxial compression test and discrete element modelling", *Computers and Geotechnics*, 67(3), 2015, PP. 94-102.
14. Tang, S., Tong, M., HU, J., He, X., "Characteristics of acoustic emission signals in damp cracking coal rocks", *Mining Science and Technology (China)*, 20(1), 2010, PP. 143-147.
15. Bogusz, A., Bukowska, M., "Stress-strain characteristics as a source of information on the destruction of rocks under the influence of load", *Journal of Sustainable Mining*, 14(1), 2015, PP. 46-54.
16. Yang, Y., Ju Y., Chen J., Gao, F., "Cracks development features and energy mechanism of dense sandstone subjected to triaxial stress", *Chinese Journal of Rock Mechanics and Engineering*, 33(4), 2013, PP. 691-698. (in Chinese)
17. Cai, M., Kaiser, P.K., Morioka, H., Minami, M., Maejima, T., Tasaka, Y., Kurose, H., "FLAC/PFC coupled numerical simulation of AE in large-scale underground excavations", *International Journal of Rock Mechanics and Mining Sciences*, 44(4), 2007, PP. 550-564.
18. Gong, Y., He, M., Wang Z., Yin, Y., "Research on time-frequency analysis algorithm and instantaneous frequency precursors for acoustic emission data from rock failure experiment", *Chinese Journal of Rock Mechanics and Engineering*, 32(4), 2013, PP. 787-799. (in Chinese)